ILASS-Americas 22nd Annual Conference on Liquid Atomization and Spray Systems, Cincinnati, OH, May 2010

Effects of Micro-Explosion on Butanol-Biodiesel-Diesel Spray and Combustion

Y. Liu[a], W. L. Cheng[b], M. Huo[b], C. F. Lee[b*] and J. Li[a]

[a] State Key Laboratory of Automobile Dynamic Simulation
Jilin University
Chang Chun City, Ji Lin Province, P. R. China

[b] Department of Mechanical Science and Engineering
University of Illinois at Urbana-Champaign
1206 West Green Street
Urbana, Illinois 61801, USA

Abstract

Blends of butanol-biodiesel-diesel were tested inside a constant volume chamber to investigate liquid spray and combustion under similar real engine working conditions. With high-speed camera and synchronized copper vapor laser, blends fuel spray penetration length is observed. Various ambient temperatures and fuel composition were investigated. There is repeatable sudden drop of spray penetration length at 800 K and 900 K, but not at 1000 K and 1200 K, supposed micro explosion occur. Further studies focus on micro explosion phenomena under non-combusting environment. High speed imaging shows that, at initial temperature 1100 K, the tip of the spray jet erupts into a plume sometime after injection for the butanol-biodiesel-diesel blend. The same is not seen with the biodiesel-diesel blend, neither at lower ambient temperature of 900 K. With biodiesel content increasing, micro explosion becomes prone excited and more violent. It is concluded that micro explosion can occurs under particular conditions for the butanol-biodiesel-diesel blend, and the results is consistent with previous theoretical study in the literature.

* Corresponding author: Chia-fon F. Lee <cflee@illinois.edu>

1. Introduction

The increasing serious fuel shortage and stringent exhaust emission regulations are urging alternative energy research and engine technology improvements. As a dominant role in diesel substitutes, biodiesel produced from animal fats, algae or non-food crop plants will evidently lower oil import for the domestic energy market [1]. Our previous studies [2, 3] shown that biodiesel produces less CO, CO_2, soot and unburned hydrocarbon, albeit a slight increase in NO_x. This is particularly important with the increasing emission restrictions. Meanwhile, alcohol is also a popular replacement to fossil fuels due to a variety of locally available feedstock. The blending of 10% ethanol in gasoline without significant modification to engine has shown encouraging results [4]. In addition, numerous articles present that blending ethanol with diesel fuel will reduce CO, NO_x and soot simultaneously [5, 6]. However, as pointed out in recent studies, n-butanol is a better alternative over ethanol because of issues with higher lubricity, solubility, heating value and longer ignition delay in diesel engines [7, 8].

Micro explosion caused by internal gasification of a liquid mixture with vastly different volatilities and boiling points, was first observed by Ivanov and Nefdov in 1965 [9]. The more volatile species inside the droplet cannot emerge to the surface sufficiently fast to compensate its vaporization rate due to finite diffusion. Therefore the temperature in some regions of the droplet is higher than the boiling points of those more volatile species. Bubbles may be generated within the droplet when the temperature is high enough to support nucleation, even though the droplet surface does not pass the boiling state. Micro explosion is the subsequent violent behavior of the droplet due to rapid growth of the bubbles. Former extensive experimental and numerical studies have been done to investigate isolated droplets behaviors. Micro explosion of freely falling droplets has been experimentally observed for miscible fuel mixtures [10, 11] as well as water-fuel emulsions [12, 13]. Wang and Law conducted a series of experiments using alcohol-alkane mixtures. Micro explosion was not significant under atmospheric pressure for conventional fuel blends. The internal bubble growth process was occupying about 10% of the whole droplet lifetime. I. Jeong and K. H. Lee reported that the micro-explosion occurred earlier and proceeded more vigorously as the ambient temperature increases. Ignition appears to be delayed apparently at lower ambient temperatures by the effect of water content. However, higher temperatures don't show serious difference in ignition delay. Proposed to describe the mechanism of micro explosion, most numerical model focused on the effects of ambient pressure and temperature, fuel composition, initial droplet size and internal phase structure of emulsified droplets on micro explosion. Some papers used superheat limit and Hill vortex theory to account the onset of micro explosion. In this model, a rapid mixing zone exits in the outer region of the moving droplet and it has very good agreement with experimental results [14]. Based upon linear stability analysis, Zeng and Lee developed a model for describing the instability of micro explosion and proposed a breakup criterion for the determination of averaged size and velocity of secondary droplets [15]. In a recent study by Lee et al. [16], micro-explosion in mixtures of ethanol-biodiesel-diesel is studied. It is reported that adding biodiesel into an ethanol-diesel blend significantly enhances micro-explosion.

Most of researches on droplet suggest that micro explosion will obviously improve liquid jet atomization and fuel/air mixture, therefore abundant emulsion fuels have been tested in conventional engine in order to reduce exhaust pollution [17, 18]. But there is no specific evidence of micro explosion existing in diesel engine and a disconnected chain existed between droplet combustion and engine application until now. So in this paper, micro explosion research on conventional spray was carried out. And different from previous fuel study which concentrated on binary blends, such as water-diesel emulsion or ethanol-diesel blend, butanol-biodiesel-diesel ternary blends fuel was tested inside optical constant volume chamber to explore spray and combustion by ambient temperature varied from 700K to 1200K.

2. Experimental procedures

2.1 Experimental setup

An optically accessible constant volume chamber is used in this study. The chamber is designed to imitate the combustion process of a diesel engine sized 110 × 67 mm, with maximum gas density of 30 kg/m^3 and utmost chamber pressure of 18 MPa. Figure 1 shows the schematic of the chamber and the liquid spray scattering. Dynasil 1100 fused silica end window is installed opposite to the injector, allowing laser beams passing and photograph taking. A Caterpillar hydraulic-actuated electronic-controlled unit injector (HEUI) is mounted at the center of the chamber head, the configuration of the injector is tabulated in Table 1. There are six nozzle orifices with 22° ascension angles. Only one of the six spray jets is examined. The cylinder wall is heated to 380 K by eight Watlow Firerod heaters, to mimic the wall temperature of a diesel engine as well as to prevent water condensation on the optical windows. Nevertheless, the oil line and fuel line inside the chamber head are kept at 350 K to simulate the situation in an actual engine and stop the evaporation of butanol before injection. A Kistler 6121 quartz pressure transducer is embedded in the chamber wall in conjunction with a 5026 dual mode differential charge amplifier. High speed images are obtained with a Phantom V7.1 non-intensified high speed digital camera, located above the optical chamber. The speed, resolution and exposure time used are 15000 fps, 256 × 256 pixels and 3 μs, respectively. The light source

is supplied by a copper vapor laser (from Oxford Lasers), with pulse repetitive frequency ranging from 4.5 kHz to 20 kHz with 10 ns exposure per pulse, that synchronizes well with the aforementioned high speed camera.

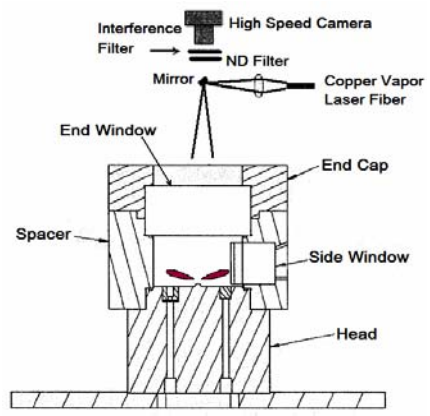

Figure 1. A schematic of the constant volume chamber

The light emitted from the fiber is condensed by an aspheric condenser lens. The laser beam enters the constant volume chamber via a reflecting mirror of 6 mm diameter placed in front of the condenser lens that could be considered as from a point source. A narrow transmittance bandwidth filter is used in order to suppress emission due to flame. Different from traditional laser diagnostics with two optical windows required, our experimental setup developed from forward illumination light extinction (FILE) method by Y. Xu and C. F. Lee, need only one end window and show favorable precision and stability [19, 20]. Furthermore, this significantly simplified the experimental setup change between fuel spray and soot formation measurement.

Table 1. Configuration of the HEUI 300A injector and the condition of fuel injections

Nozzle style	VCO
No. of Nozzle Holes	6
Spray angle	140°
Orifice Diameter	0.145 mm
Injection Pressure	134 MPa
Injection Duration	3.5 ms
Fuel Quantity	120 mm^3
Fuel Temperature	350 K

The pre-injection condition in a diesel engine is simulated by burning a lean mixture of acetylene (C_2H_2), oxygen and nitrogen to setup the high temperature and pressure condition. The amount of oxygen is adjusted according to the required oxygen density after the premixed burn, simulating various levels of exhaust gas recirculation (EGR). A typical operation condition for diesel engine without EGR is chosen: 21% oxygen (by volume) and density of 14.8 kg/m^3. The HEUI injector and high speed camera are simultaneously triggered once the chamber pressure (or temperature) reaches the desired value. Several initial temperatures in chamber are considered in this study: 800 K, 900 K, 1000 K and 1200 K, covering both low-temperature combustion (at about 800 K) and conventional combustion (1000 K to 1200 K) in diesel engines.

2.2 Light scattering for liquid penetration length and dispersion angle measurement

The liquid spray penetration length and dispersion angle are determined by a computational code. Each frame of the high speed movie, captured by the camera, is processed sequentially. The working principle of liquid spray light scattering is the different reflective rate from the liquid droplets and its surrounding background. Stronger incident light is being reflected from the liquid spray to the camera than the "darker" ambient. Therefore, the liquid jet can be highlighted in the resulting images. A low reflective background is needed for the better Mie scattering signal. Therefore, the camera will observe stronger reflection of the laser beam from spray, then jet penetration can be determined from each of the images obtained.

The injector orifice is marked at the top center of each of the images. The computer code searches along the centerline of the liquid jet to locate the pixel with highest intensity. Note that all pixels with intensity below a preset threshold are neglected. The threshold is determined from a cumulative intensity histogram for each film image set. In this histogram two peaks appear, one is corresponding to the ambient gas region with low intensity level and another is corresponding to liquid spray region with high intensity levels. A threshold intensity midway between the two peaks in the cumulative histogram was chosen. The liquid penetration length is defined as the distance between the injector orifice and the pixel with intensity first falling below the preset threshold along the centerline of the liquid jet. The dispersion angle is defined by taking the arctangent of half maximum radial spray width divided by axial location of the spray width [21].

2.3 Mathematical Formulations

Simulations of fuel injection and combustion processes are done to predict combustion pressure and heat release rate in this study. A modified version of KIVA 3V Release 2 computer code [22] is used for all numerical works. The computational package is capable of conducting three-dimensional modeling of the evaporation, mixing, ignition, combustion and pollutants formation processes. First of all, the fuel library in KIVA is extended to include properties of n-butanol and biodiesel for application with the two fuels. Properties for biodiesel are generated by the software BDProp [23]

while those for butanol are estimated from correlations found in Yaw et al. [24]. In addition to expanding the fuel library, the multi-component evaporation model developed and verified by Zeng and Lee, is inserted into the program, allowing accurate modeling of a blended fuel, such as the ternary mixture of butanol-biodiesel-diesel. Its accuracy on spray evaporation and combustion had been verified in various publications by the group [25].

2.4 Fuel Properties

The ternary mixture of diesel, soybean biodiesel and n-butanol is being studied. Selected thermo-physical and chemical properties of pure substances are tabulated in Table 2 from official analysis report of supplier companies. Comparison with traditional ethanol, n-butanol has higher solubility and cetane number in diesel fuel. And biodiesel is known to act as an additive or emulsifier due to its potential to improve the solubility of alcohol in diesel fuel over a wide range of temperatures and blend properties. So butanol-biodiesel-diesel ternary blends keep a homogeneous miscible liquid with no particles or crystals in the entire experiment. Note that n-butanol has the lowest boiling point (390 K), and highest volatility, since micro-explosion might occur in a mixture of butanol-biodiesel-diesel.

Table 2. Selected thermo-physical and chemical properties for n-butanol, soybean biodiesel and diesel

	n-Butanol	Biodiesel	Diesel
Density[g/cm^3] (at 25°C)	0.81	0.885	0.837
Kinematic Viscosity [mm^3/s] (at 40°C)	3.1	4.11	2.42
Cetane Number	17	47.1	50.1
Boiling Point[K]	390	627	593
Lower Heating Value [MJ/kg]	33.2	38.4	45.8
Heat of Vaporization [kJ/kg]	592	320.2	270
Stoichiometric A/F Ratio	11.1	12.7	14.6
Oxygen Content[%]	19	10	N/A
Surface Tension [dyne/cm] (at 20°C)	24.0	32.5	27.5
Vapor Pressure[mm-Hg] (at 20°C)	5	0.4	~ 0

The addition of n-butanol to diesel fuel decreased fuel density and surface tension, but this could be compensated for by adding biodiesel. Therefore B10S10D80 (10% n-butanol by volume, 10% soybean biodiesel and 80% diesel) and B5S15D80 which has properties close to diesel are examined in this study for spray and combustion. Afterwards, to extend the understanding of the micro explosion with bio-fuel, higher n-butanol and biodiesel blend ratio in ternary mixture fuels are used to investigate without combustion.

3. Results and discussion

3.1 Measured and predicted pressure, heat release rate

Figures 2 show the predicted and measured pressure and heat release rates for the butanol-biodiesel-diesel blends. Very strong premixed combustion is observed at 800 K and 900 K initial temperatures, signified by the dual-peaked heat release rate curves from experimental measurements. At initial ambient temperature of 1000 K, a weak premixed combustion is observed, indicated by the small spike in the heat release rate curve at about 2.7 ms. However, at initial temperature of 1200 K, mixing controlled combustion is the only combustion mode observed. The peak heat release rates decreased with the increase of ambient temperature for both blends considered in this study. The presence of n-butanol seems to strengthen the premixed combustion. Comparing between the 5% n-butanol blend results against the 10% n-butanol blend for 800 K case, it is observed that lower n-butanol leads to lower peak combustion pressure. The maximum combustion pressure for the 10% n-butanol blend is about 10% higher than that for the 5% n-butanol blend.

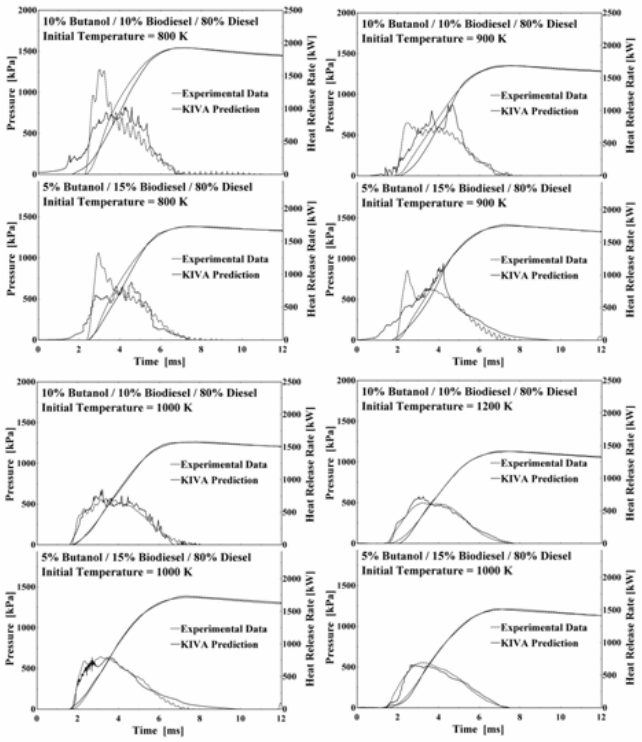

Figure 2. Pressure and heat release rate at different initial temperature

KIVA predictions compare well with experimental data in high temperature, which indicates that KIVA can give accurate results for evaporation, mixing, and combustion calculations. KIVA correctly predicted the tail end of the heat release rate and pressure at initial temperatures of 800 K and 900 K, but it fails to predict the strong premixed combustion observed in experimental

measurements. So the failure of KIVA prediction in low temperature case is because some phenomena happened in experiment which was not modeled by KIVA, like micro-explosion. To explain the discrepancy between the computations and experiments at 800 and 900 K, the attention is turned to the spray penetration.

3.2 Spray penetration & micro-explosion speculation

The measured spray jet penetrations for the B5S15D80, B10S10D80 and B0S20D80 blends are average values of five measuring shown in Figure 3 for various initial temperatures.

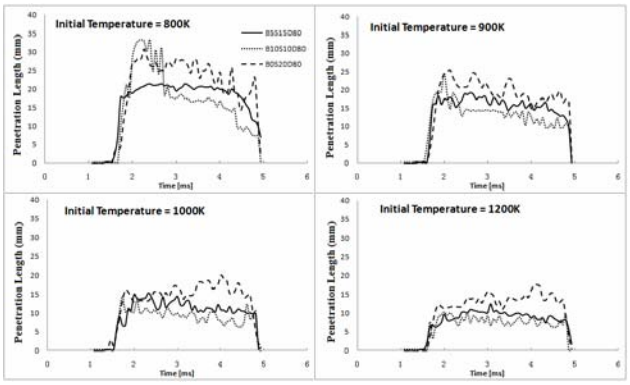

Figure 3. Spray jet penetration at initial temperatures of 800K to 1200K

The fuel jet become observable at about 1.45 ms and reaches the maximum penetration depth at about 0.21 ms later for all the four temperatures shown. Faster evaporation and shorter ignition delay at elevated temperature causes the penetration depth to reduce with higher initial temperature. From Table 2, n-Butanol has the lowest boiling point among the three components. The viscosity of n-butanol is also lower than biodiesel. Hence, replacing biodiesel by n-butanol reduces the penetration length of a biodiesel-diesel mixture, which shown from Figure 3, as droplet breakup is easier with lower viscosity. Therefore, the average droplet size reduces, promoting fuel evaporation. The 0% n-butanol blend has the highest liquid jet penetration while the penetration of the 10% n-butanol blend is the shortest. There is a sudden drop observed in spray penetration with the 10% n-butanol blend at about 3 ms with ambient temperatures of 800 K and 900 K, this unusual observation is detected repeatedly during liquid jet penetration measuring. The phenomenon is not observed at high ambient temperatures of 1000 K and 1200 K. For the latter cases, the spray penetration remains 15 mm at 1000 K and 10 mm at 1200 K for the duration of the spray.

Figure 4 shows the spray penetration and heat release rate for the 10% n-butanol blend at initial ambient temperature of 800 K. There is a sudden decrement in penetration length immediately after auto-ignition when the chamber temperature at that instant is about 1100 K. This spray penetration drop can be seen from Figure 5. Compared with B0S20D80 stable injection state, there is black gaseous phenomenon blocked downstream of the liquid jet. It might be related to micro-explosion, so further examinations are performed to study the effects of n-butanol on spray dynamics. In order to eliminate the effect of combustion on spray jet, amount of excess oxygen content is set to zero. This ensures that further comparisons on spray penetrations are not distorted by the combustion process of the fuel.

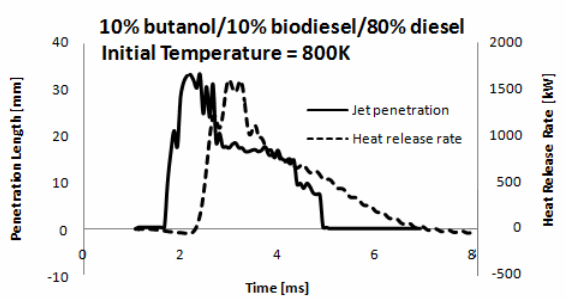

Figure 4. Spray jet penetration and heat release rate for 10% butanol-10% biodiesel blend at 800 K

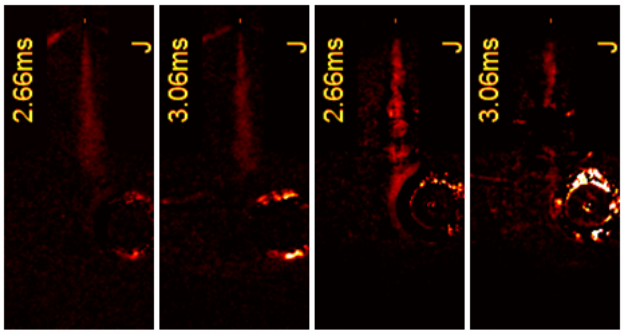

Figure 5. Spray jet images for B0S20D80 (left) and B10S10D80 (right) blends at 800 K

3.3 Visual micro explosion investigation in spray

The evolution of liquid jets at initial 900 K and 1100 K ambient without combustion are shown in Figures 6 and 7, respectively. At 900 K initial ambient temperature, both B10S10D80 and B0S20D80 blends keep similar spray course. But the liquid spray jets behave in a vastly different manner for the two fuels at 1100 K in Figure 7. The liquid jet for the 0% n-butanol blend keeps a normal jet for the duration of injection. However, at 1.86 ms, the tip for the 10% n-butanol blend erupts into a plume. The plume detached itself from the spray jet, which explains the sudden drop in former penetration measurement, per the definition of spray penetration in this study (i.e. for a continuous dense spray in pixels measured from the injector tip). This observation continues until 2.06 ms, note that the plume at spray tip is no longer observed in the image at 2.13 ms and later, because fuel evaporation

consumes amount of thermal in the chamber and reduced ambient temperature cannot sustain micro explosion occurring.

The comparison of dispersion angle is more obvious at 1100 K than at 900 K. At both 900 K and 1100 K, the spray jet angle of the 10% n-butanol blend is larger than that of the fuel without n-butanol. Not only the surface tension of n-butanol is less than that of biodiesel that is negatively related to the dispersion angle, but also micro explosion located outer layer extends the spray boundary.

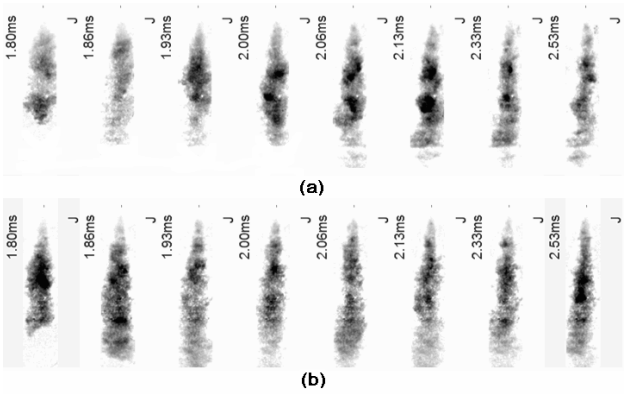

Figure 6. Spray jet penetration image of ambient temperatures of 900 K: (a) B10S10D80; (b) B0S20D80

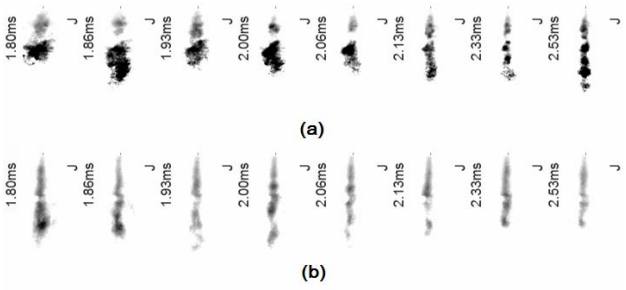

Figure 7. Spray jet penetration image of ambient temperatures of 1100 K: (a) B10S10D80; (b) B0S20D80

With the significant differences in volatilities and boiling points among n-butanol, biodiesel and diesel, micro-explosion can occur in a butanol-biodiesel-diesel mixture. Recently, our numerical study on micro-explosion has shown that increasing n-butanol and biodiesel contents in ternary fuel is an effective way to induce micro-explosion due to the enlarged differences in volatilities and boiling point among the components. Therefore 30% of n-butanol and various biodiesel blends from 20% to 60% are examined in following research.

As the initial ambient temperature is 900 K, B30S60D10 blend shows violent micro explosion located spray tip from 2.0 ms to 2.39 ms in Fig. 8 (a). The micro explosion is strong enough to eject fragments of torn droplet tip to several millimeters away from the main spray body, and expand the spray tip and dispersion angle, cause the spray shape irregular. Because of fast evaporation and secondary atomization due to micro explosion, some gaseous regions in liquid spray are hard to be detected by high speed camera. For B30D40S30 and B30D20S50 blends, fuel spray keep normal behavior as B10S10D80 in Fig. 6, no micro explosion occurring.

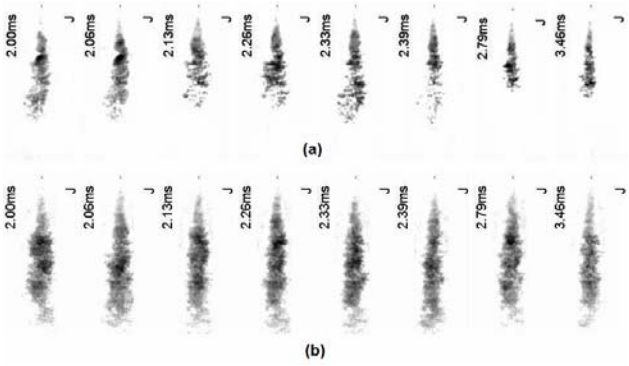

Figure 8. Spray jet penetration image of ambient temperatures of 900 K: (a) B30S60D10; (b) B30S40D30

With ambient temperature increasing, the start of micro explosion advances at 1000 K for B30S60D10 blend, but the intensity and duration become lower in Fig. 9 (a). It is first time to detect micro explosion phenomena for B30S40D30 blend fuel. There is still no obvious micro explosion taking place for B30S20D50 blend.

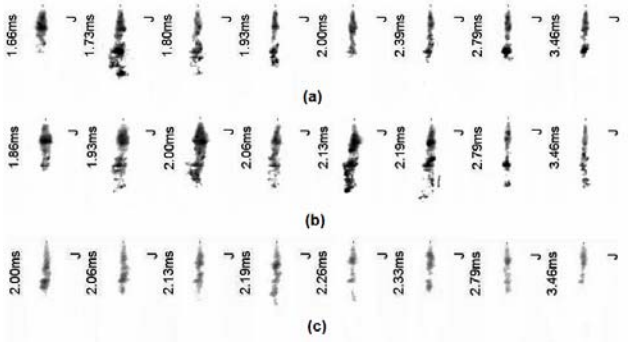

Figure 9. Spray jet penetration image of ambient temperatures of 1000 K: (a) B30S60D10; (b) B30S40D30; (c) B30S20D50

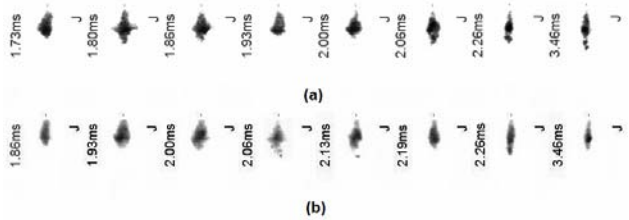

Figure 10. Spray jet penetration image of ambient temperatures of 1050 K: (a) B30S40D30; (b) B30S20D50

At 1050 K initial temperature condition, faster generated fuel vapor surrounding liquid jet retard liquid

jet penetration, that results in greater dispersion angle contrastively shown in Fig. 9 (c) and Fig. 10 (b). The micro explosion appears on both sides instead of spray tip, especially cross-shaped spray detected at 1.80 ms in Fig. 10 (a) and at 2.06 ms in Fig. 10 (b).

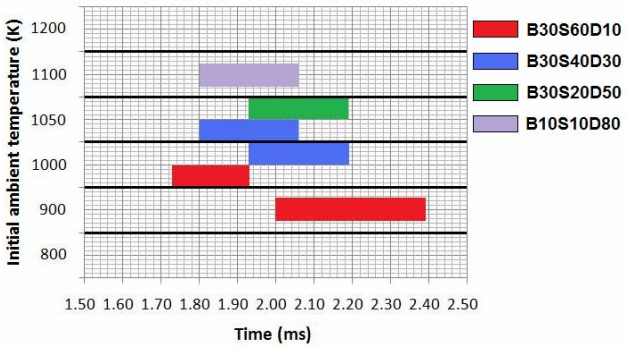

Figure 11. Onset time and duration of micro explosion at varied initial temperature for different blends fuel

Figure 11 shows the onset time and the duration of micro explosion at various initial temperatures for different blends fuel. For 30% n-butanol and 60% biodiesel blend in Fig. 11, micro explosion is detected from 2.00 ms to 2.39 ms at 900 K ambient temperature, with initial temperature increased to 1000 K, the onset time of micro explosion advanced because higher temperature difference between liquid spray and external environment makes bubbles faster grow inside droplets. On the other hand, the liquid jet penetration length turns to be short at relative higher ambient temperature due to rapid atomization and vaporization which consume more thermal. Without fuel combustion supporting, n-butanol dots cannot achieve the limit of superheat, so the duration of micro explosion became short. There is no micro explosion existed neither below 900 K nor above 1000 K initial temperature for B30S60S10 blend. B30S40D30 blend fuel obtains the similar trend as B30S60D10 fuel at relative higher initial temperature condition. Micro explosion was observed only at 1050 K for B30S20D50 blends. For B30S60D10 and B30S40D30, the content of n-butanol is constant, at the 1000 K ambient condition, reducing biodiesel content (from 60% to 40%) instead of diesel, the time appeared micro explosion retards due to lessening the difference in volatilities among component species. It is also detected at 1050 ambient temperature for B30S40D30 and B30S20D50 blend. Compared to high butanol, high biodiesel content fuel, B10S10D80 blend only was detected micro explosion appearance at 1100 K initial ambient temperature and had the same micro explosion duration to B30S20D50 blend.

Therefore, it concluded that micro explosion can be enhanced by adding less high-volatile liquid into fuel blend, and it matched well with our former mathematical formulations of micro explosion [16].

4. Summary and conclusions

The effects of n-butanol and biodiesel blended in diesel fuel on spray dynamics and combustion are examined in this study. B10S10D80 blend fuel presented disruption of liquid jet penetration length at 800 K and 900 K initial ambient temperature. This repeatable unusual trend induces distinct premixed combustion and the highest heat release peak that did not match very well with KIVA 3V Release 2 simulation which had been verified against many experiments in various publications. This unusual phenomenon is not caused by liquid evaporation alone and suppose micro explosion existing. Therefore the second part of the study focused on the investigation of the visualization of spray micro-explosion isolating the effect of combustion. High speed imaging shows that, for the non-combusting case, at 1100 K, the tip of the spray jet erupts into a plume sometime after injection for the butanol-biodiesel-diesel blend. The same is not seen with the biodiesel-diesel blend, neither at lower ambient temperature of 900 K. And then, more different blend rates fuel are investigated on various initial temperature precondition, starting time and duration of micro explosion.

It is concluded that micro-explosion can occur under particular conditions for the butanol-biodiesel-diesel blends. The detailed conclusions are as follows:

(1) Shortened spray jet penetration is observed when ambient temperature is higher, due to faster liquid evaporation at elevated temperature. Adding n-butanol to the binary mixture of biodiesel-diesel also reduces spray penetration due to the higher volatility of n-butanol.

(2) Adding n-butanol content to biodiesel-diesel fuel is able to cause micro explosion which will distinctly enhances premixed combustion process and heat release rate under certain initial ambient temperature conditions. Micro explosion is hard to be detected when the butanol blend rate is lower than 10%,

(3) Keep n-butanol content constant, with biodiesel content increasing, micro explosion appears at relative low initial ambient temperature.

(4) With ambient temperature increasing, the starting time of micro explosion advanced. At the same initial ambient temperature condition, difference in volatilities among component species positively effects the starting time of micro explosion.

(5) The downstream of fuel jet become divergent and fragmentary when micro-explosion occurs. This also shortens liquid jet penetration length. Fuel evaporation is enhanced in local region that is hard to be recorded by light scattering method.

Acknowledgements

This work was supported in part by the U.S. Department of Energy (DOE) Grant No. DE-FC26-05NT42634 by DOE GATE Centers of Excellence Grant No. DE-FG26-05NT42622, by China Scholarship Council

and by Caterpillar Inc.. The authors thank Incobrasa Industries, Ltd. for their supply of biodiesel. The support of the quality control manager Kerry Fogarty and plant manager Sergio Baruffi from Incobrasa Industries, Ltd. is greatly appreciated. This work was performed using the equipment in the University of Illinois, and the support of the university staffs is greatly appreciated.

References

[1] R. Burrett and M. Eckhart, Renewable Energy Policy Network for the 21st Century, (2007)
[2] T. Fang and C. F. Lee, Proc. Combust. Inst. 32 (2009) 2785-2792.
[3] T. Fang, Y. C. Lin, T. M. Foong and C. F. Lee, Fuel 88 (2009) 2154-2162.
[4] H. S. Yücesu, T. Topgül, C. Çinar and M. Okur, Applied Thermal Engineering, 26 (2006) 2272-2278.
[5] X. Li, X. Qiao, L. Zhang, J. Fang, Z. Huang and H. Xia, Renewable Energy, 30 (2005) 2075-2084.
[6] P. Satgé De Caro, Z. Mouloungui, G. Vaitilingom, and J. Ch. Berge, Fuel 80 (2001) 565-574.
[7] A. Chotwichien, A. Luengnaruemitchai, S. Jai-In, Fuel 88 (2009) 1618-1624.
[8] X. C. Lü, J. G. Yang, W. G. Zhang and Z. Huang, Fuel 83 (2004) 2013-2020.
[9] V. M. Ivanov and P. I. Nefdov, NASA TT F-258 (1965).
[10] J. C. Lasheras, A. C. Fernandez-Pello and F. L. Dryer, Combust. Sci. Tech. 22 (1980) 195-209.
[11] C. H. Wang and C. K. Law, Combustion and Flame 59 (1985) 53-62.
[12] J. C. Lasheras, A. C. Fernandez-Pello and F. L. Dryer, Combust. Sci. Tech., 21 (1979) l-4.
[13] I. Jeong, K. H. Lee and J. Kim, Journal of Mechanical Science and Technology, 22(2008)148-156
[14] H. Z. Sheng, Z. P. Zhang and C. K. Wu, International Symposium COMODIA, 90(1990)275-280
[15] Y. Zeng and C. F. Lee, Proceedings of the Combustion Inst., 31(2007) 2185-2193
[16] C. F. Lee, K. T. Wang and W. L. Cheng, SAE Paper 2008-01-0937 (2008)
[17] D. H. Qi, H. Chen and C. F. Lee, Energy Fuels, 24(2010)652-663
[18] W. B. Fu, J. S. Gong and L. Y. Hou, Chinese Science Bulletin, 51(2006)1261-1265
[19] Y. Xu and C. F. Lee, Applied Optics, 45 (2006) 2046-2057.
[20] Y. Xu and C. F. Lee, SAE Paper, (2006)01-1415.
[21] J. D. Naber and D. L. Siebers, SAE Paper, (1996)960034
[22] A. Amsden, KIVA-3V: a Block-Structured KIVA Program for Engines with Vertical or Canted Valves, Los Alamos Natl. Lab. Rep. LA-13313-MS (1997)
[23] W. Yuan, A. C. Hansen, M. E. Tat, J. H. Van Gerpen and Z. Tan, Transactions of the ASAE 48 (2005) 933-939
[24] C. Yaws, Chemical Properties Handbook, McGraw-Hill, New York (1998)
[25] Y. Zeng and C. F. Lee, J. of Propulsion and Power 16 (2000) 964-973